Development/Plasticity/Repair

NMDA Receptor GluRε/NR2 Subunits Are Essential for Postsynaptic Localization and Protein Stability of GluRζ1/NR1 Subunit

Manabu Abe,[1,5]* Masahiro Fukaya,[2]* Takeshi Yagi,[3] Masayoshi Mishina,[4,5] Masahiko Watanabe,[2] and Kenji Sakimura[1,5]

[1]Department of Cellular Neurobiology, Brain Research Institute, Niigata University, Niigata 951-8585, Japan, [2]Department of Anatomy, Hokkaido University School of Medicine, Sapporo 060-8638, Japan, [3]KOKORO Biology Group and Core Research for Evolutional Science and Technology, Laboratories for Integrated Biology, Graduate School of Frontier Biosciences, Osaka University, Suita 565-0871, Japan, [4]Department of Molecular Neurobiology and Pharmacology, Graduate School of Medicine, University of Tokyo, Tokyo 113-0033, Japan, and [5]Solution Oriented Research for Science and Technology, Japan Science and Technology, Tokyo 113-0033, Japan

In NMDA receptors, GluRε/NR2 subunits strictly require the GluRζ1/NR1 subunit to exit from endoplasmic reticulum (ER) to the cell surface *in vitro* and to the postsynapse *in vivo*, whereas C terminus-dependent self-surface delivery has been demonstrated for the GluRζ1 subunit *in vitro*. To test whether this leads to C terminus-dependent self-postsynaptic expression in neurons *in vivo*, we investigated the GluRζ1 subunit in cerebellar granule cells lacking two major GluRε subunits, GluRε1/NR2A and GluRε3/NR2C. In the mutant cerebellum, synaptic labeling for the GluRζ1 subunit containing the C2 (GluRζ1-C2) or C2′ (GluRζ1-C2′) cassette was reduced at mossy fiber–granule cell synapses to the extrasynaptic level. The loss was not accompanied by decreased transcription and translation levels, increased extrasynaptic labeling, or ER accumulation. Quantitative immunoblot revealed substantial reductions in the mutant cerebellum of GluRζ1-C2 and GluRζ1-C2′. The most severe deficit was observed in the postsynaptic density (PSD) fraction: mutant levels relative to the wild-type level were 12.3 ± 3.3% for GluRζ1-C2 and 17.0 ± 4.6% for GluRζ1-C2′. The GluRζ1 subunit carrying the C1 cassette (GluRζ1-C1) was, although low in cerebellar content, also reduced to 12.7 ± 3.5% in the mutant PSD fraction. Considering a trace amount of other GluRε subunits in the mutant cerebellum, the severe reductions thus represent that the GluRζ1 subunit, by itself, is virtually unable to accumulate at postsynaptic sites, regardless of C-terminal forms. By protein turnover analysis, the degradation of the GluRζ1 subunit was accelerated in the mutant cerebellum, being particularly rapid for that carrying the C2 cassette. Therefore, accompanying expression of GluRε subunits is essential for postsynaptic localization and protein stability of the GluRζ1 subunit.

Key words: **NMDA receptor; mossy fiber–granule cell synapse; immunohistochemistry; immunoblot; protein turnover; cerebellum; knock-out mouse**

Introduction

The NMDA-selective glutamate receptor is involved in activity-dependent changes of synaptic efficacy, which underlie synapse development, synaptic plasticity, and learning and memory (Mayer and Westbrook, 1987; Bliss and Collingridge, 1993). NMDA receptors are composed of GluRζ1/NR1 and GluRε/NR2 subunits (Seeburg, 1993; Nakanishi and Masu, 1994; Mori and Mishina, 1995). The GluRζ1 subunit is encoded by a single gene but exists as several splice variants. The GluRε subunit is composed of four members (GluRε1–ε4 or NR2A–2D) and determines functional and spatiotemporal diversities of NMDA receptors (Kutsuwada et al., 1992; Meguro et al., 1992; Monyer et al., 1992; Watanabe et al., 1992).

Heteromeric configuration of NMDA receptors has been evidenced from *in vitro* experiments. First, active NMDA receptors are obtained only when the GluRε subunit is expressed together with the GluRζ1 subunit (Meguro et al., 1992; Monyer et al., 1992). Second, binding sites for agonist glutamate and coagonist glycine are shared between GluRε and GluRζ1 subunits (Hirai et al., 1996; Laube et al., 1997). Third, GluRζ1 and GluRε subunits interact differentially with various cytoskeletal and synaptic molecules thought to regulate receptor transport, localization, and dynamics (Kornau et al., 1995; Niethammer et al., 1996; Wyszynski et al., 1997; Ehlers et al., 1998; Setou et al., 2000). Fourth, GluRε subunits require cotransfection of the GluRζ1 subunit for their exit from the endoplasmic reticulum (ER) to the cell surface (McIlhinney et al., 1996, 1998). Indeed, when the *GluRζ1* gene is deleted in hippocampal pyramidal cells *in vivo*, GluRε subunits

Received Oct. 3, 2003; revised June 15, 2004; accepted June 18, 2004.

This work was supported by Special Coordination Funds for Promoting Science and Technology and Grants-in-Aid for Scientific Research (A, B) and for Scientific Research on Priority Areas, all provided by the Ministry of Education, Culture, Sports, Science and Technology, Japan. We thank E. Kushiya, K. Kitayama (Brain Research Institute, Niigata University, Niigata, Japan), and M. Sanbo (National Institute for Physiological Sciences, Okazaki, Japan) for technical assistance and R. Natsume (Core Research for Evolutional Science and Technology, Solution Oriented Research for Science and Technology) for mouse breeding.

*M.A. and M.F. contributed equally to this work.

Correspondence should be addressed to Dr. Masahiko Watanabe, Department of Anatomy, Hokkaido University School of Medicine, Sapporo 060-8638, Japan. E-mail: watamasa@med.hokudai.ac.jp.

DOI:10.1523/JNEUROSCI.1261-04.2004

 0270-6474/04/247292-13$15.00/0

are retained in the somatic ER and disappear from the postsynaptic site (Fukaya et al., 2003).

Four different C termini of the GluRζ1 subunit are generated by optional usage of the C1 exon cassette and by alternative usage of the C2/C2′ cassettes (Sugihara et al., 1992; Yamazaki et al., 1992; Hollmann et al., 1993). These variants differ in potentiation by PKC (Tingley et al., 1993), regional expression in the brain (Laurie et al., 1995), interaction with cytoskeletal filaments (Ehlers et al., 1998; Lin et al., 1998; Matsuda and Hirai, 1999), and cell surface expression (Ehlers et al., 1995). Of these variants, higher self-surface expression is shown for the GluRζ1 subunit with the C2′ tail than that with the C2 tail, and also for the GluRζ1 subunit lacking the C1 cassette than that carrying it (Okabe et al., 1999). Furthermore, alternative C2/C2′ usage is activity dependent and controls ER export and synaptic delivery of NMDA receptors (Mu et al., 2003).

This *in vitro* evidence prompted us to test whether this leads to C terminus-dependent self-postsynaptic expression of the GluRζ1 subunit in neurons *in vivo*, by producing cerebellar granule cells lacking two major GluRε subunits, GluRε1/NR2A and GluRε3/NR2C. Here, we show that, when accompanying GluRε subunits are lacking, postsynaptic localization is impaired for the GluRζ1 subunit with any C-terminal cassettes. Moreover, the ablation of GluRε subunits causes rapid degradation of the GluRζ1 subunit, particularly that carrying the C2 cassette. Therefore, accompanying GluRε subunits are essential for postsynaptic expression and protein stability of the GluRζ1 subunit in neurons *in vivo*.

Materials and Methods

Production of the GluRε3 and GluRε1/ε3 knock-out mice. A genomic DNA clone, λGRE3T1–12 (Nagasawa et al., 1996), carrying the *GluRε3* gene was used to construct a targeting vector. A 0.7 kb *Hin*dIII-*Not*I fragment containing the transmembrane segment M4 was replaced with a 1.3 kb *Eco*RI-*Bam*HI fragment from pGK2Neo (Yagi et al., 1993) containing the pgk-neo cassette. A 4.0 kb *Sal*I-*Not*I fragment from pPauDT3 (Yanagawa et al., 1999) was used for negative selection. TT2 embryonic stem (ES) cells were transfected by the linearized vector, and the targeted clones were identified by G418 selection, PCR, and Southern blot hybridization using the three probes shown in Figure 1*A*. Generation of germ-line chimeras and production of homozygous GluRε3 knock-out (GluRε3-KO) mice were performed in the same manner as described (Sakimura et al., 1995). To produce mutant mice defective in both GluRε1 and GluRε3 subunits, GluRε3-KO mice were mated with GluRε1-KO mice, as reported previously (Sakimura et al., 1995).

Sections. Under deep pentobarbital anesthesia (100 mg/kg body weight), wild-type and mutant mice at 1 month of age were perfused transcardially with the following fixatives: 4% paraformaldehyde in 0.1 M sodium phosphate buffer (PB), pH 7.4, for light microscopic immunohistochemistry and histology (paraffin sections, 5 μm in thickness; microslicer sections, 50 μm); 4% paraformaldehyde/0.1% glutaraldehyde in 0.1 M PB, pH 7.4, for post-embedding immunogold (Lowicryl sections, 100 nm); or 2% paraformaldehyde/2% glutaraldehyde in 0.1 M sodium cacodylate buffer, pH 7.4, for electron microscopy (ultrathin Epon sections, 70 nm) and granule cell count (semithin Epon sections, 1 μm). Before Epon embedding, cerebellar slices were further postfixed with 1% osmium tetroxide in 0.1 M sodium cacodylate buffer, pH 7.4, for 2 hr, stained in block with 2% uranyl acetate for 1 hr, and dehydrated in graded alcohols. Brains for *in situ* hybridization were freshly obtained for cyrostat sections (20 μm).

In situ *hybridization. In situ* hybridization analysis was performed using subunit-specific antisense oligonucleotides for the GluRε1 subunit (oligoε1E), GluRε3 subunit (oligoε3M4C), and GluRζ1 subunit (oligoζ1A). Oligoε1E and oligoε3M4C are complementary to the nucleotide residues 1862–1906 of the GluRε1 subunit cDNA (Meguro et al., 1992) and 2525–2570 of the GluRε3 subunit cDNA (Kutsuwada et al., 1992), respectively. Oligoζ1A was reported previously (Watanabe et al., 1993). Probe labeling and procedures for *in situ* hybridization were done as reported previously (Watanabe et al., 1993). After washing, sections were exposed to BioMax film (Eastman Kodak, Rochester, NY) for 3 weeks. The relative gray density was obtained by scanning x-ray film autoradiograms and measuring with NIH Image software (version 1.61).

Antibody. We raised polyclonal antibodies against the C1 and C2′ cassettes of the GluRζ1 subunit in the rabbit and guinea pig, respectively, using synthetic peptides (CDPKKKATFRAITSTLASSFKRRRSSKDT for the C1 and CQYHPTDITGPLNLSDPSVSTVV for the C2′) conjugated to keyhole limpet hemocyanin. Procedures for immunization and antibody purification were reported previously (Watanabe et al., 1998). We also used rabbit anti-GluRζ1-C2 (Yamada et al., 2001), rat monoclonal anti-GluRζ1-N (GluRζ1-pan) (Yamada et al., 2001), rabbit anti-GluRε1C (Watanabe et al., 1998), rabbit anti-GluRε2C (Watanabe et al., 1998), rabbit anti-GluRε3C (Yamada et al., 2001), rabbit and guinea pig anti-postsynaptic density (PSD)-95 (Fukaya and Watanabe, 2000), guinea pig anti-vesicular glutamate transporter VGluT1 (Miyazaki et al., 2003), rabbit anti-vesicular GABA transporter VGAT (Miyazaki et al., 2003), rabbit anti-synaptophysin (Fukaya and Watanabe, 2000), and goat anti-calreticulin (Santa Cruz Biotechnology, Santa Cruz, CA) antibodies. All antibodies were used at the concentration of 0.5–1 μg/ml, unless noted otherwise.

To check the specificity of GluRζ1 antibodies, the GluRζ1 subunit tailed with the C1–C2 cassettes (NR1–1) or with the C2′cassette only (NR1–4) was expressed under the control of the human elongation factor 1α promoter. HEK293 cells were transfected using Lipofectamine reagent (Invitrogen, Carlsbad, CA) and lysed 2 d later by the addition of harvest buffer (1 mM EGTA, pH 8.1, 1 mM EDTA, pH 7.9, 1% TritonX-100, and 1 mM PMSF). For control immunohistochemistry, GluRζ1 antibodies were preabsorbed with C2 or C2′ antigen peptides (50 μg/ml each) by overnight incubation at 4°C.

Immunohistochemistry. Before conventional immunohistochemical incubation, paraffin sections were subjected to pepsin pretreatment, which is essential for immunohistochemical detection of NMDA receptor subunits and the PSD-95/synapse-associated protein (SAP)-90 protein family (Watanabe et al., 1998; Fukaya and Watanabe, 2000; Yamada et al., 2001; Oshima et al., 2002). After treatment with 1 mg/ml pepsin (Dako, Carpinteria, CA) in 0.2N HCl at 37°C for 10 min, sections were immunoreacted successively with rabbit or guinea pig primary antibodies overnight, biotinylated secondary antibodies for 1 hr, and streptoavidin–peroxidase for 30 min, using a Histofine SAB-PO(R) kit (Nichirei, Tokyo, Japan). Immunoreaction was visualized with DAB, and photographs were taken using a light microscope (AX-70; Olympus, Tokyo, Japan).

For confocal laser-scanning microscopy (Fluoview; Olympus), pepsin-treated paraffin sections were incubated first with GluRζ1-C2 or GluRζ1-C2′ antibody overnight, biotinylated goat anti-rabbit or anti-guinea pig IgG for 1 hr, and streptoavidin–peroxidase for 30 min, followed by visualization using the Tyramide Signal Amplification kit [TSA Fluorescein System (green); NEN Life Science, Boston, MA]. Then, sections were incubated with guinea pig or rabbit PSD-95 antibody overnight, followed by a 2 hr incubation with Cy3-labeled donkey anti-guinea pig or anti-rabbit IgG (1:200; Jackson ImmunoResearch, West Grove, PA) or with 10 μM propidium iodide for 10 min (Molecular Probes, Eugene, OR). Double immunofluorescence for VGluT1 and VGAT was also conducted using microslicer sections, followed by a 2 hr incubation with a mixture of Cy3- or FITC-labeled, species-specific secondary antibodies (Jackson ImmunoResearch).

Procedures for post-embedding immunogold were the same as reported previously (Fukaya and Watanabe, 2000). Ultrathin sections from three wild-type and three mutant mice were immunoreacted overnight with GluRζ1-C2 or GluRζ1-C2′ antibody (10 μg/ml) and then with colloidal gold (10 nm) conjugated with anti-rabbit or anti-guinea pig IgG (British Biocell International, Cardiff, UK) for 2 hr. Grids were stained with 2% uranyl acetate for 10 min. The number of gold particles was counted on the synaptic and extrasynaptic membranes, respectively, of asymmetrical synapses between mossy fiber terminals and granule cell dendrites.

Morphological analysis. Parasagittal microslicer sections were stained with hematoxylin and used for cerebellar histology. Using the sections,

areal measurement of the granular layer was performed by taking cerebellar images with an AX-70 light microscope equipped with a CCD camera (Sensys 1401; Nippon Roper, Tokyo, Japan) and by calculating using MetaMorph software (Nippon Roper). Semithin Epon sections stained with Mayer's hematoxylin were used for granule cell counting, as follows. The numerical density (Nv) of granule cells was obtained by the point-counting method of Weibel (1979) and using the equation: $Nv = 1/\beta \times N_A{}^{1.5}/Vv^{0.5}$, as reported previously (Kakizawa et al., 2000). N_A and Vv are the visible profile count of granule cell nuclei or their volume density in the granular layer, respectively, whereas β is a dimensionless shape coefficient defined here as 1.38 by assuming that granule cell nuclei are spherical.

For analysis of cerebellar synapses, electron micrographs were taken from the middle-third depth of the granular layer with an H7100 electron microscope (Hitachi, Tokyo, Japan). The mean length of PSD at mossy fiber–granule cell synapses was measured by IPlab software (Nippon Roper).

Western blot analysis. For quantitative Western blot analysis, five cerebella of each genotype were pooled for one experiment. The cerebella were homogenized in 10 volumes of sucrose buffer (0.32 M sucrose, 5 mM EDTA, 1 mM PMSF, 1 μM pepstatin A, and 2 μM leupeptin) and centrifuged at 700 × *g* for 10 min to obtain the postnuclear fractions (homogenates). The synaptosomal and PSD fractions were prepared as described previously (Carlin et al., 1980). To obtain the PSD fraction, the synaptosomal fraction was further treated with 0.5% Triton X-100 for 15 min on ice and then centrifuged at 81,600 × *g* for 1 hr. The resultant pellets were resuspended in 40 mM Tris-HCl, pH 8.0. To obtain the light membrane fraction (P3 fraction) in a separate procedure, the S2 fraction prepared from a cerebellum was centrifuged at 165,000 × *g* for 2 hr, and the resultant pellets were resuspended with the sucrose buffer.

The determination of protein concentrations was made by the method of Lowry et al. (1951). Protein samples were fractionated by 7% SDS-PAGE and electroblotted onto nitrocellulose membranes (Schuleicher & Schuell, Dassell, Germany). The blot was immunoreacted with primary antibodies and visualized using the ECL chemiluminescence detection system (Amersham, Bucks, UK). Signal intensities of immunoreaction were measured digitally. To normalize signal intensities on each blot, equal amounts of control protein samples were loaded simultaneously and defined as standard signals. Representative data from three to five experiments are shown in the figures.

Pulse labeling of cultured cerebellar cells. Cultures of cerebellar granular cells were prepared as described by Fujikawa et al. (2000), with minor modifications. Briefly, cerebella obtained from the wild-type or GluRε1-KO mice at 6–7 d of age were treated with 0.2% trypsin for 15 min at 37°C. Cells were centrifuged and suspended in MEM-Hanks (Invitrogen) supplemented with 10 mM HEPES-NaOH, pH 7.2, 1 μM arabinosylcytosine, and 10% FCS and were plated on polyethyleneimine-coated culture plates at a density of 2.4×10^5 cells/cm^2. One day after plating, 20 mM KCl was added to the medium. All experiments were performed on days 7–8 *in vitro*. Northern blot analysis of GluRζ1 mRNA was performed by hybridization of total RNA using a ^{32}P-labeled GluRζ1 cDNA probe (nucleotide residues 203–758). An immunoblot was performed as described above. Pulse labeling and immunoprecipitation were performed as described by Huh and Wenthold (1999), with minor modifications. Cells were incubated for 30 min at 37°C in methionine- and cysteine-free medium supplemented with 10% FCS and then pulse labeled with 125 μCi/ml [^{35}S]methionine and [^{35}S]cysteine in depletion medium for 30 min. After 30 min, cells were washed immediately with cold PBS, harvested, and solubilized with buffer containing 2% SDS by incubating for 3 min at 90°C. Ten micrograms of GluRζ1-N antibody were used for immunoprecipitation. Immunoprecipitated proteins were eluted and subjected to SDS-PAGE and immunoblot. After an immunoblot, radioactivity of the pulse-labeled GluRζ1 subunit was analyzed by FUJIX Bioimage Analyzer (BAS2000; Fuji Film, Tokyo, Japan).

Protein synthesis inhibition. Anisomycin (Sigma, St. Louis, MO) was dissolved in 1N HCl and diluted in 0.9% saline. The pH was adjusted to 4.5 with 1N NaOH. Mice were given subcutaneous injections of 150 mg of anisomycin/kg of body weight or an equivalent volume of vehicle. At this dose, anisomycin has been shown to inhibit protein synthesis in the brain by >90% during the first 2 hr and by >60% during the next 2 hr (Lattal and Abel, 2001). Four hours after injection, homogenate samples were prepared from the cerebellum, and an immunoblot was performed as described above.

Results

Production of GluRε1/ε3-KO mice

The *GluRε3* gene locus in murine TT2 ES cells was disrupted by homologous recombination using a targeting vector containing an 8.5 kb fragment of GluRε3 subunit genomic DNA, in which the exon encoding the transmembrane segment M4 was replaced with the neomycin phosphotransferase gene (Fig. 1*A*). From ES cells electroporated with the vector DNA, we selected 1210 clones in medium containing G418, from which two clones with correct targeting were identified by PCR and Southern blot hybridization analyses. Germ-line chimeric mice were generated by injecting the clone 8-88-3. Heterozygous progenies were intercrossed, and their offspring were genotyped by Southern blot analysis with three probes (Fig. 1*B*). Homozygous GluRε3 mutant (GluRε3-KO) mice were then crossed with the GluRε1-KO mouse (Sakimura et al., 1995) to obtain the double knock-out (GluRε1/ε3-KO) mouse. The GluRε3-KO and GluRε1/ε3-KO mice were viable, grew normally, and were fertile. However, the GluRε1/ε3-KO mouse showed mild impairment in motor coordination when tested on the rotating rod at high speeds (data not shown), as reported previously (Ebralidze et al., 1996; Kadotani et al., 1996).

In situ hybridization

By *in situ* hybridization, the absence of GluRε1 and/or GluRε3 mRNAs in the respective mutant brains was confirmed with ^{33}P-labeled probes against the deleted sequences (Fig. 1*C*, top and middle). No genotypic differences were detected in overall distribution of GluRζ1 mRNA in the brain (Fig. 1*C*, bottom). The relative OD in the cerebellar granular layer was quantified using a single x-ray film, to which all hybridized sections had been exposed. At the transcription level, no compensatory upregulation was seen for the GluRε1 subunit in the absence of the *GluRε3* gene, and vice versa (Fig. 1*D*, left and middle) ($n = 3$; Student's t test; $p > 0.05$ for each). Moreover, GluRζ1 mRNA levels in the granular layer showed no significant differences among the four types of mice (Fig. 1*D*, right) ($p > 0.05$ for each). Thus, the gene knock-out of the GluRε1 subunit, GluRε3 subunit, or both does not affect the transcription levels of the remaining NMDA receptor subunits.

Specificity of GluRζ1-C2, -C2′, and -C1 antibodies

To examine the effect on C-terminal variants of the GluRζ1 subunit, the specificity of C2, C2′, and C1 cassette antibodies was assessed by immunoblot and immunohistochemical analyses (Fig. 2). In the cerebellum, all three antibodies recognized protein bands at 120 kDa. The band detected by the C2 or C2′ antibody was broad and apparently consisted of multiple sub-bands in the cerebellar homogenate (Fig. 2*A*, Cb). In contrast, the band recognized by the C1 antibody was detected in the cerebellar PSD fraction (Fig. 2*A*, Cb) but not in the homogenate (data not shown), suggesting low contents of the C1 cassette in the cerebellum (see also Fig. 6*A*). The C2, C2′, and C1 antibodies selectively recognized protein bands in HEK293 cells transfected with plasmid encoding NR1–1 (GluRζ1 subunit tailed with C1–C2), NR1–4 (that tailed with C2′), or NR1–1, respectively (Fig. 2*A*). Preincubation of these antibodies with their immunizing peptides completely abolished these protein bands, whereas the bands were similarly detected by preincubation with the other (nonimmunizing) peptides (data not shown). These results indi-

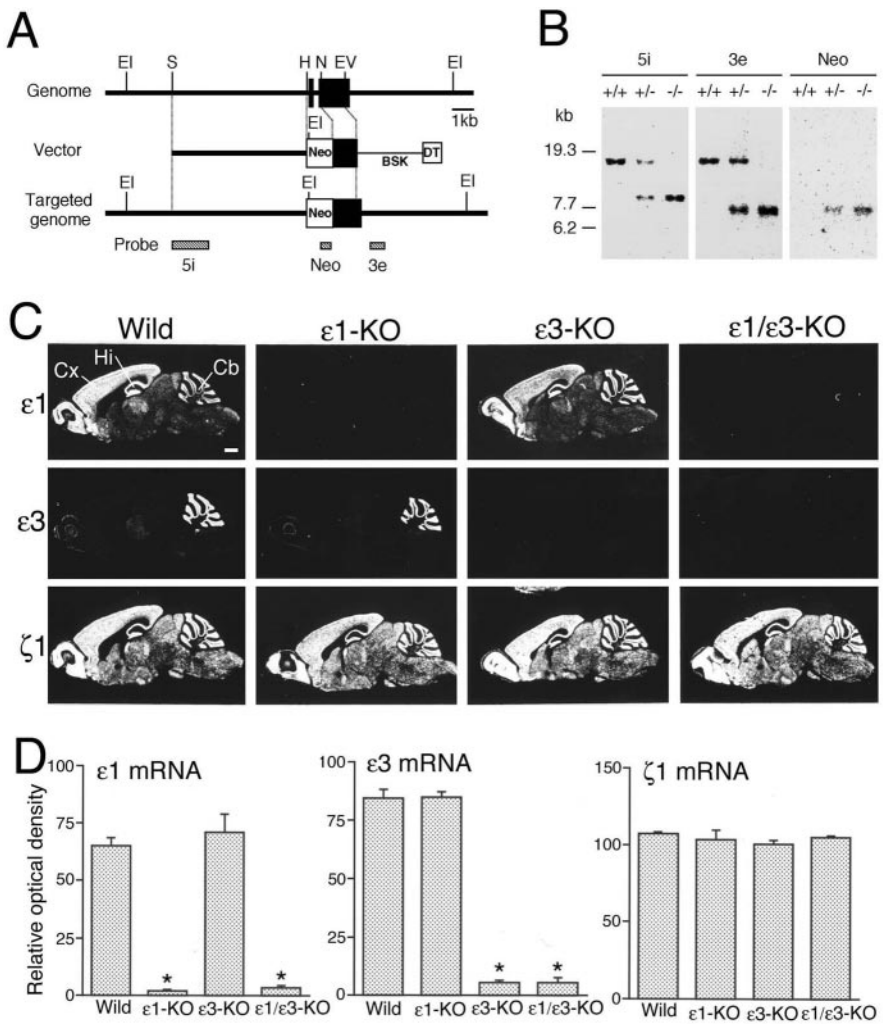

Figure 1. Production of mutant mice defective in NMDA receptor *GluRε1* and/or *GluRε3* subunit genes. *A*, Schematic representation of genomic DNA, targeting vector, and disrupted gene of the GluRε3 subunit. *B*, Southern blot analysis of *Eco*RI-digested genomic DNA using three different probes indicated in *A*. *C*, *In situ* hybridization analysis for GluRε1, GluRε3, and GluRζ1 mRNAs in the wild-type, GluRε1-KO, GluRε3-KO, and GluRε1/ε3-KO brains. *D*, Semiquantitative evaluation of transcription levels for GluRε1 (left), GluRε3 (center), and GluRζ1 (right) mRNAs in the granular layer of the cerebellum (mean ± SD). The asterisks indicate statistically significant differences between wild-type and mutant mice (Student's *t* test; $p < 0.001$). BSK, Plasmid pBluescript; Cb, cerebellum; Cx, cerebral cortex; DT, diphtheria toxin gene; EI, *Eco*RI; EV, *Eco*RV; H, *Hin*dIII; Hi, hippocampus; N, *Not*I; S, *Sal*I. Scale bar, (in *C*) 1 mm.

cate that the three antibodies are specific to the C2, C2′, and C1 cassettes, respectively, and have no cross-reactivity to the others.

By immunohistochemistry, C2 and C2′ antibodies yielded characteristic labelings in the adult mouse brain that were similar but not identical to each other (Fig. 2*B*,*E*). The immunolabelings were abolished with the use of antibodies preincubated with immunizing peptides (Fig. 2*C*,*G*), but not with nonimmunizing ones (Fig. 2*D*,*F*). Thus, the C2 and C2′ antibodies are specific in use for immunohistochemistry as well as for immunoblot. However, the C1 antibody failed to produce reliable immunohistochemical labeling and was used for immunoblot analysis only.

Hereafter, the GluRζ1 subunit detected by the C2, C2′, and C1 antibodies is referred to as GluRζ1-C2, GluRζ1-C2′, and GluRζ1-C1, respectively.

Immunohistochemistry

Alterations at the protein level were examined by immunohistochemistry at the light microscopic (Figs. 3, 4) and electron microscopic (Fig. 5) levels.

Light microscopic immunohistochemistry for GluRζ1-C2 and GluRζ1-C2′

To minimize experimental fluctuation in light microscopic immunohistochemistry, pairs of wild-type and mutant brains were embedded in single paraffin blocks, and hence all immunohistochemical procedures were applied to the section pairs under the same conditions.

In the wild-type brain, the highest immunostaining for GluRζ1-C2 was detected in the hippocampal CA1 region (Fig. 3*A–C*, top brains). High levels were also observed in the cerebral cortex, olfactory bulb, caudate–putamen, hippocampal CA3 region, dentate gyrus, and cerebellar granular layer, whereas the level in the thalamus was low to moderate. In contrast, GluRζ1-C2′ was highest in each subregion of the hippocampus and also high in the cerebral cortex, thalamus, and cerebellar granular layer, whereas it was low in the caudate–putamen (Fig. 3*D*, top brain). These patterns of immunostaining are consistent with the reported distributions of C2 and C2′ cassette mRNAs, respectively (Laurie et al., 1995). When compared with the wild-type brain, GluRζ1-C2 in the cerebellar granular layer was reduced mildly in the GluRε1-KO mouse (Fig. 3*A*, bottom brain), reduced severely in the GluRε3-KO mouse (Fig. 3*B*, bottom brain), and almost negative in the GluRε1/ε3-KO mouse (Fig. 3*C*, bottom brain). This was also true for GluRζ1-C2′ (Fig. 3*D*, bottom brain).

By nuclear counterstaining with propidium iodide (Fig. 3*E*,*I*, red) or hematoxylin (Fig. 4*A*,*E*, blue), GluRζ1-C2 and GluRζ1-C2′ were shown in the wild-type mouse to be located in oval or polygonal masses between granule cells (Figs. 3*E*,*I*, green, 4*A*,*E*, brown). These immunopositive structures were well overlapped with postsynaptic density protein PSD-95 (Fig. 3*G*,*K*, red), indicating that GluRζ1-C2 and GluRζ1-C2′ are accumulated extensively in synaptic glomeruli. In mutants, immunoreactivity in synaptic glomeruli was progressively reduced in the order of wild-type>GluRε1-KO>GluRε3-KO>GluRε1/ε3-KO mice (Fig. 4*A–D*, GluRζ1-C2; *E–H*, GluRζ1-C2′). In the GluRε1/ε3-KO mouse, both variants were almost undetectable in synaptic glomeruli (Fig. 3*F*,*H*,*J*,*L*). Thus, parallel with GluRε subunit ablation, immunohistochemical visibility of GluRζ1-C2 and GluRζ1-C2′ was lost from cerebellar synaptic glomeruli, where granule cell dendrites form excitatory and inhibitory synapses with mossy fibers or Golgi cell axons, respectively.

Postembedding immunogold for GluRζ1-C2 and GluRζ1-C2′

The subcellular localization was examined by postembedding immunogold (Fig. 5). In the wild-type mouse, gold particles representing GluRζ1-C2 or GluRζ1-C2′ were observed in the postsynaptic membrane at asymmetrical synapses in contact with huge mossy fiber terminals (Fig. 5*A*,*B*), whereas they were hardly

detected at this type of synapse in the GluRε1/ε3-KO mouse (Fig. 5*C*,*D*). We evaluated the difference by comparing the mean number of immunogold particles per micrometer of the synaptic (junctional) and extrasynaptic (nonjunctional) membranes. The mean number of gold particles for GluRζ1-C2 on the synaptic membrane was 5.55 ± 1.22 in the wild-type mouse (mean ± SEM; $n = 3$; 101 synapses examined), whereas it was significantly lowered to 0.35 ± 0.08 in the GluRε1/ε3-KO mouse ($n = 3$; 60 synapses; Student's t test; $p < 0.05$), the latter density being similar to the extrasynaptic density in both the wild-type and GluRε1/ε3-KO mice (Fig. 5*E*). As for GluRζ1-C2′, the mean number on the synaptic membrane was 3.91 ± 0.66 in the wild-type mouse ($n = 3$; 88 synapses) and 0.60 ± 0.20 in the GluRε1/ε3-KO mouse ($n = 3$; 78 synapses), showing significant reduction ($p < 0.05$) (Fig. 5*F*). Thus, synaptic localization of the GluRζ1 subunit was significantly reduced to the extrasynaptic level in the GluRε1/ε3-KO mouse, regardless of the C2/C2′ form. Despite the severe synaptic loss, no significant increase of the extrasynaptic density was evident in the GluRε1/ε3-KO mouse ($p > 0.05$ for each variant).

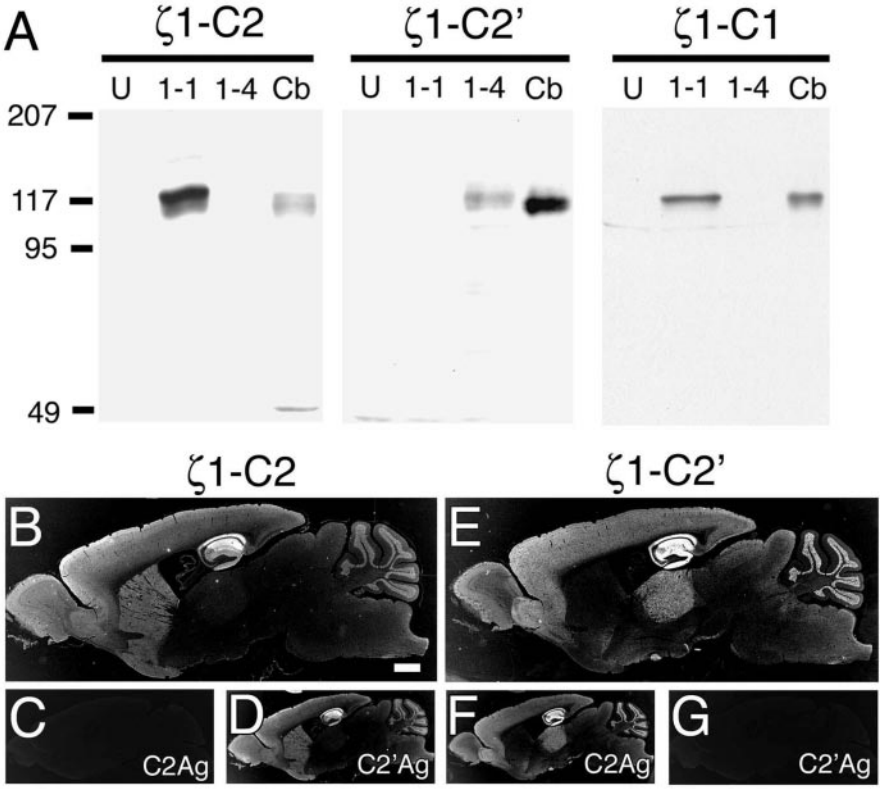

Figure 2. Specificity of GluRζ1-C2, GluRζ1-C2′, and GluRζ1-C1 antibodies. *A*, Immunoblot using untransfected HEK293 cells (U), cells transfected with GluRζ1 containing the C1 and C2 cassettes (NR1–1), cells transfected with GluRζ1 lacking the C1 but containing the C2′ cassette (NR1–4), and cerebellar proteins (Cb). Cerebellar homogenates (30 μg) were loaded for GluRζ1-C2 and GluRζ1-C2′, whereas cerebellar proteins in the PSD fraction (10 μg) were loaded for GluRζ1-C1. *B–G*, Immunoperoxidase staining for GluRζ1-C2 (*B–D*) and GluRζ1-C2′ (*E–G*) subunits. Antibodies were preincubated without (*B*, *E*) or with C2 (*C*, *F*) and C2′ (*D*, *G*) antigen peptides. Scale bar, 1 mm.

In our previous study using mutant mice lacking the GluRζ1 subunit, GluRε1 and GluRε2/NR2B subunits abnormally accumulate in perikarya of hippocampal pyramidal cells as electron-dense granules in the ER lumen (Fukaya et al., 2003). In the present study, we also searched for such somatic accumulation and intracisternal granule formation. However, we could not find any somatic accumulation of the GluRζ1 subunit in GluRε1/ε3-deficient granule cells by light microscopy (Fig. 3*F*,*J*) and postembedding immunogold (data not shown).

GluRε subunits and PSD-95

Changes of the GluRε1 subunit (Fig. 4*I–L*), GluRε3 subunit (Fig. 4*M–P*), and PSD-95 (Fig. 4*Q–T*) were examined in the granular layer. Compared with the wild-type mouse (Fig. 4*I*,*M*), glomerular staining was reduced for the GluRε1 subunit in the GluRε3-KO mouse (Fig. 4*K*) and for the GluRε3 subunit in the GluRε1-KO mouse (Fig. 4*N*), despite their normal transcription levels (Fig. 1*C*,*D*). In contrast, no differences were seen in the distribution and levels of PSD-95 among the four mouse types (Fig. 4*Q–T*). These results suggest that genetic ablation of given GluRε subunits has affected synaptic expression of the remaining GluRε subunits as well.

Immunoblot

Then, we performed immunoblot analysis to biochemically characterize the effect of GluRε subunit ablation on cerebellar content and intracellular distribution of the GluRζ1 subunit (Fig. 6, Table 1). All immunoblotting data were quantified by three independent experiments ($n = 3$), except for GluRζ1-C2′ in the homogenate, synaptosomal fraction, and PSD fraction of the wild-type mouse (five experiments; $n = 5$) and for GluRζ1-C1 in the PSD fraction of the wild-type mouse (four experiments; $n = 4$). When necessary, different amounts of protein samples were loaded in lanes for accurate comparison (see figure legends).

C-terminal exon usage in the wild-type cerebellum

The relative abundance of the GluRζ1 subunit was compared between the cerebrum (cerebral cortex) and cerebellum, using homogenates from the wild-type mouse (Fig. 6*A*). The total GluRζ1 content, as assessed using the GluRζ1-pan antibody raised against the N-terminal region (GluRζ1-N antibody) (Yamada et al., 2001), was three times lower in the cerebellum than in the cerebrum: the cerebellum/cerebrum ratio was calculated as 1.00 ± 0.10/3.55 ± 0.43. Compared with the total GluRζ1 subunit, the ratio was further reduced for GluRζ1-C2 (1.00 ± 0.02/11.76 ± 0.50), whereas it was comparable for GluRζ1-C2′ (1.00 ± 0.22/3.44 ± 0.41). Despite the presence of a strong band in the cerebrum, GluRζ1-C1 was not detected in the cerebellar homogenate, even with an increased amount of proteins loaded (Fig. 6*A*). These results suggest that the C-terminal form of the cerebellar GluRζ1 subunit is characterized by relatively higher usage of the C2′ alternative cassette than the C2 cassette, and by much lower usage of the C1 optional cassette, compared with the cerebral GluRζ1 subunit.

The relative abundance of the C2 and C2′ cassettes in the cerebellum was determined. First, NR1–1 and NR1–4 proteins expressed in HEK cells were standardized by graded dilution of these samples and by immunoblot detection with GluRζ1-pan antibody. Then, using the standardized NR1–1 and NR1–4 sam-

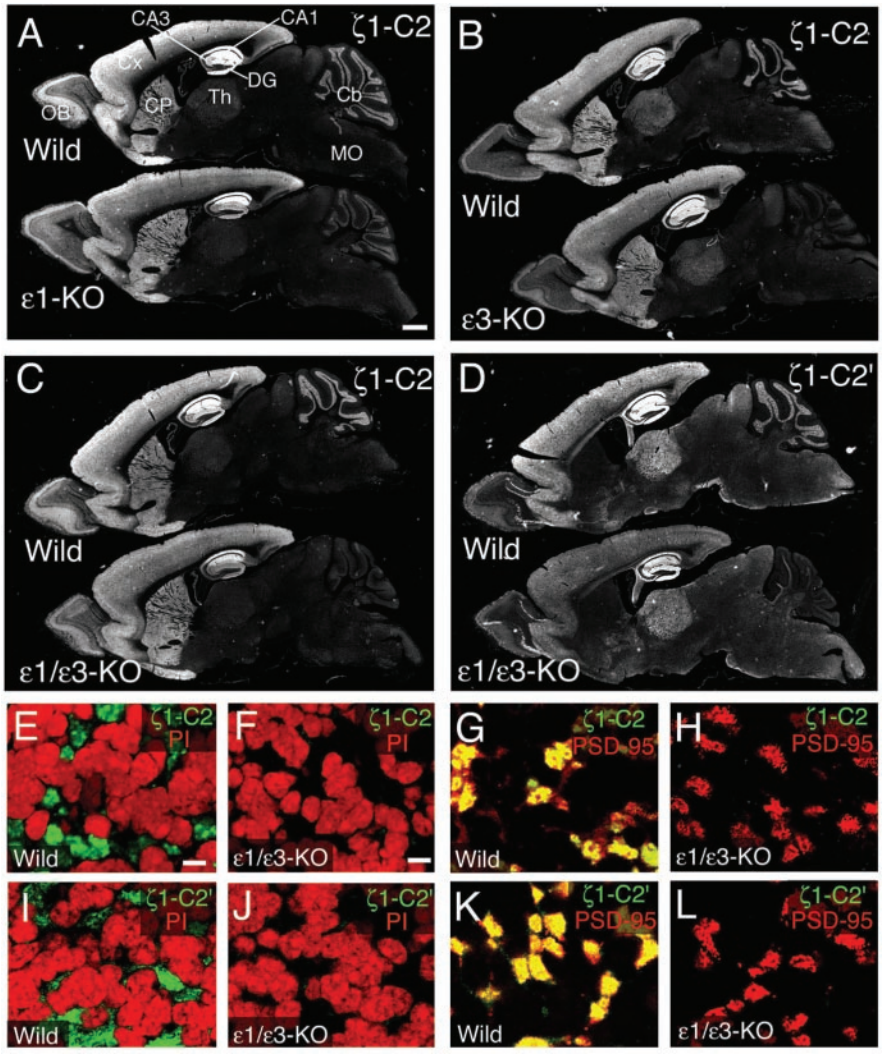

Figure 3. Immunohistochemical alterations of GluRζ1-C2 (*A–C*, *E–H*) and GluRζ1-C2′ (*D*, *I–L*) in mutant mice lacking GluRε subunits. *A–D*, Pairs of wild-type (top) and mutant (bottom; *A*, GluRε1-KO; *B*, GluRε3-KO; *C*, *D*, GluRε1/ε3-KO) brains. Photographs are negative images printed directly from preparates stained by immunoperoxidase using diaminobenzidine as a chromogen. *E*, *F*, *I*, *J*, Double fluorescence for the GluRζ1 subunit (green) and nuclear staining with propidium iodide (PI; red) in the cerebellar granular layer of the wild-type (*E*, *I*) and GluRε1/ε3-KO (*F*, *J*) mice. *G*, *H*, *K*, *L*, Double immunofluorescence for the GluRζ1 subunit (green) and PSD-95 (red) in the cerebellar granular layer of the wild-type (*G*, *K*) and GluRε1/ε3-KO (*H*, *L*) mice. CA1 and CA3, CA1 and CA3 regions of the hippocampus; Cb, cerebellum; CP, caudate–putamen; Cx, cerebral cortex; DG, dentate gyrus; MO, medulla oblongata; OB, olfactory bulb; Th, thalamus. Scale bars: *A*, 1 mm; *E*, *F*, 5 μm.

ples as a reference, the intensity of the GluRζ1-C2 or GluRζ1-C2′ band in a given amount of cerebellar homogenates was corrected for comparison. Consequently, the relative abundance in cerebellar homogenates was estimated to be 39.1 ± 3.2% for GluRζ1-C2 and 66.0 ± 11.0% for and GluRζ1-C2′. Taking an undetectable level of GluRζ1-C1 in cerebellar homogenates, the major splice form in the cerebellum is thus the GluRζ1 subunit having the C2′ cassette (i.e., NR1–4) with that having the C2 cassette (NR1–2) in the second abundance, whereas the GluRζ1 subunit having the C1 cassette (NR1–1 and NR1–3) is considerably low in the cerebellum.

Total GluRζ1 subunit

Changes in cerebellar contents of the total GluRζ1 subunit were compared between the wild-type and mutant mice (Fig. 6*B*, Table 1). The total GluRζ1 subunit was progressively reduced to 74.0 ± 15.8% in the GluRε1-KO mice, 69.6 ± 13.2% in the GluRε3-KO mice, and 60.3 ± 10.2% in the GluRε1/ε3-KO mice [mean ± SEM; Student's *t* test; $p < 0.05$, compared with the wild-type level (100 ± 8.4%)] (Fig. 6*B*). Taking the virtual loss of postsynaptic immunogold labeling (Fig. 5), the GluRζ1 subunit remaining in the mutant cerebella was unexpectedly high, suggesting altered intracellular distribution in the GluRε-deficient cerebella. To address this issue, subcellular fractionation was used for immunoblot analysis on GluRζ1-C2, GluRζ1-C2′, and GluRζ1-C1.

GluRζ1-C2 and GluRζ1-C2′

Cerebellar contents of GluRζ1-C2 and GluRζ1-C2′ were also reduced in the mutant mice (Fig. 6*B*,*D*,*G*; Table 1). GluRζ1-C2 was reduced to 70.2 ± 7.1% in the GluRε1-KO mice ($p < 0.05$), 66.5 ± 10.1% in the GluRε3-KO mice ($p < 0.05$), and 41.4 ± 0.4% in the GluRε1/ε3-KO mice [$p < 0.01$, compared with wild-type GluRζ1-C2 (100 ± 3.2%)], and GluRζ1-C2′ was reduced to 73.1 ± 6.4% in the GluRε1-KO mice, 69.1 ± 8.6% in the GluRε3-KO mice, and 53.0 ± 5.6% in the GluRε1/ε3-KO mice [$p < 0.05$, compared with wild-type GluRζ1-C2′ (100 ± 9.6%)].

Analysis of the P3 or microsomal fraction, which contains organelles including the ER, Golgi apparatus, and synaptic mitochondria, revealed a significant decrease in the GluRε1/ε3-KO mouse for GluRζ1-C2 (60.1 ± 7.4%; $p < 0.05$) and GluRζ1-C2′ [64.1 ± 2.7%; $p < 0.05$, compared with wild-type levels (100 ± 7.4% and 100 ± 12.5%, respectively)] (Fig. 6*C*). Because no significant changes were observed for resident ER protein calreticulin on the same blotted membrane (Fig. 6*C*), this reduction was judged to be specific to the GluRζ1 subunit.

Then, the synaptic GluRζ1 subunit was assessed by comparative examination using the cerebellar synaptosomal and PSD fractions (Fig. 6*D*,*G*; Table 1). The quality of these fractions was confirmed in all four genotypes, by the enrichment of the presynaptic protein synaptophysin in the synaptosomal fraction, the enrichment of postsynaptic protein PSD-95 in the PSD fraction, and the lack of synaptophysin in the PSD fraction (Fig. 6*D*). In the synaptosomal fraction, GluRζ1-C2 was reduced to 62.4 ± 7.6% in the GluRε1-KO mouse, 71.5 ± 12.6% in the GluRε3-KO mouse, and 34.2 ± 5.6% in the GluRε1/ε3-KO mouse [$p < 0.05$, compared with the wild-type synaptosomal fraction (100 ± 23.0%)]. Reduction was more pronounced in the PSD fraction: the GluRζ1-C2 level was 46.6 ± 10.5% in the GluRε1-KO mouse, 35.0 ± 17.7% in the GluRε3-KO mouse, and 12.3 ± 3.3% in the GluRε1/ε3-KO mouse [$p < 0.05$, compared with the wild-type PSD fraction (100 ± 23.3%)]. Similar results were obtained for GluRζ1-C2′ (Fig. 6*D*). In the synaptosomal fraction, GluRζ1-C2′ was reduced to 47.9 ± 12.8% in the GluRε1-KO mouse ($p <$

0.05), 60.5 ± 17.2% in the GluRε3-KO mouse, and 26.3 ± 4.3% in the GluRε1/ε3-KO mouse [$p < 0.01$, compared with the wild-type synaptosomal fraction (100 ± 10.5%)]. In the PSD fraction, the level of GluRζ1-C2′ was 46.2 ± 20.6% in the GluRε1-KO mouse, 25.1 ± 5.3% in the GluRε3-KO mouse, and 17.0 ± 4.6% in the GluRε1/ε3-KO mouse [$p < 0.05$, compared with the wild-type PSD fraction (100 ± 24.4%)]. Thus, synaptic GluRζ1-C2 and GluRζ1-C2′ were progressively reduced according to GluRε subunit ablation, with the most severe deficit in the PSD fraction

GluRζ1-C1

The fact that GluRζ1-C1 was detectable in the PSD fraction but not in homogenages suggests its low contents in the cerebellum and its enriched localization in the postsynapse (Figs. 2*A*, 6*E*; Table 1). GluRζ1-C1 in the PSD fraction was also reduced severely in the mutant cerebella: 55.2 ± 4.3% in the GluRε1-KO mouse ($p < 0.05$), 36.6 ± 5.7% in the GluRε3-KO mouse ($p < 0.05$), and 12.7 ± 3.5% in the GluRε1/ε3-KO mouse [$p < 0.01$, compared with the wild-type PSD fraction (100 ± 14.5%)] (Fig. 6*E*,*G*). Therefore, GluRζ1-C1 also requires the presence of GluRε subunits for its successful postsynaptic expression.

GluRε subunits and other synaptic molecules

Consistent with immunohistochemical results, a significant reduction was also observed for cerebellar contents of the GluRε1 subunit in the GluRε3-KO mouse [67.8 ± 7.5%; $p < 0.05$, compared with the wild-type homogenate (100 ± 4.9%)] and for the GluRε3 subunit in the GluRε1-KO mouse [67.9 ± 7.0%; $p < 0.05$, compared with the wild-type homogenate (100 ± 2.9%)] (Fig. 6*B*). Therefore, the ablation of one GluRε subunit has also reduced cerebellar contents of the other endogenous GluRε subunit.

Because the GluRε2 subunit is highly expressed in immature granule cells during the early postnatal period (Watanabe et al., 1992), we examined whether compensatory changes occurred for GluRε2 subunit expression in the mutant cerebellum at 1 month of age (Fig. 6*F*). In the wild-type mouse, the GluRε2 subunit was prominently expressed in the cerebral cortex, whereas it was low but still detectable in the cerebellum, as reported previously (Takahashi et al., 1996). No significant difference was observed in the cerebellar level of the GluRε2 subunit between the wild-type (100.0 ± 20.6%) and GluRε1/ε3-KO mice (107.9 ± 33.2%; $p > 0.05$).

Regardless of the substantial reduction of the GluRζ1 subunit, no significant changes were seen for PSD-95 and synaptophysin in the whole cerebellar homogenate, synaptosome fraction, and PSD fraction (Fig. 6*B*,*D*). Rather, levels of PSD-95 showed an increasing tendency in mutants, but the changes were not statistically significant.

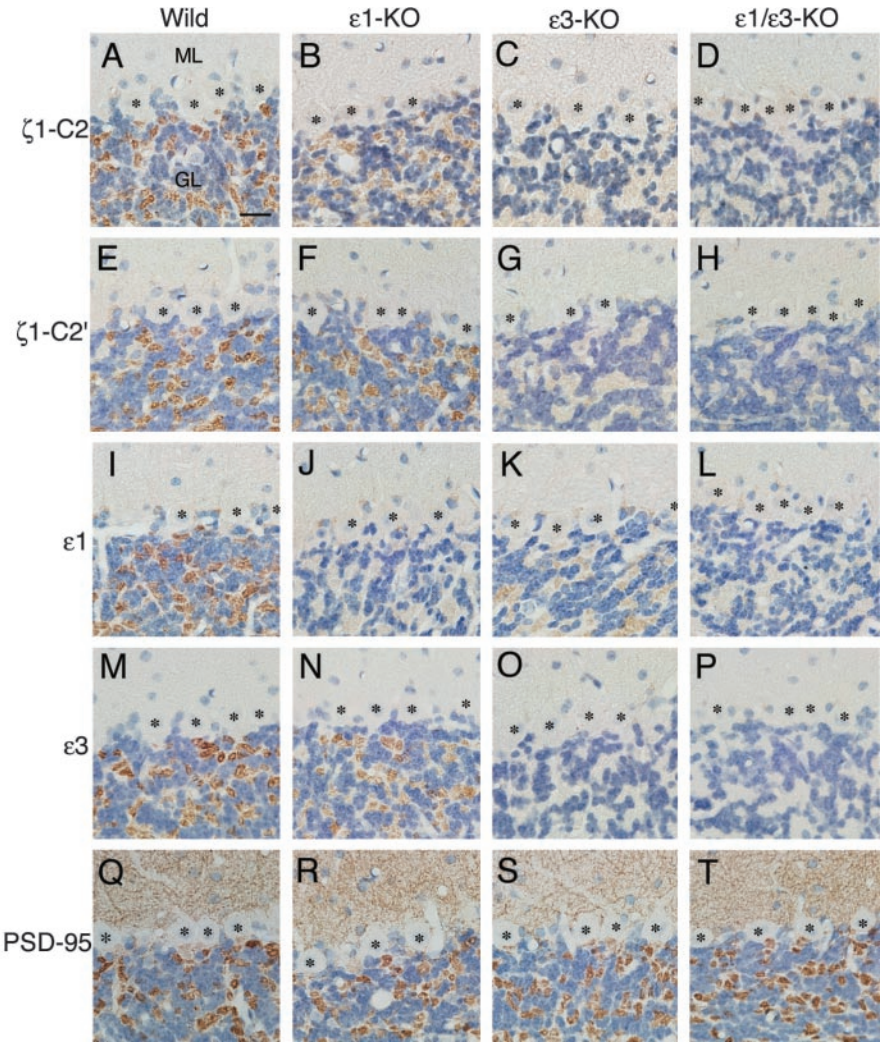

Figure 4. Immunoperoxidase for the cerebellar cortex using antibodies specific to GluRζ1-C2 (*A–D*), GluRζ1-C2′ (*E–H*), GluRε1 (*I–L*), GluRε3 (*M–P*), and PSD-95 (*Q–T*). Note a gradual reduction of immunoreactivities for the GluRζ1 subunit from *A* to *D* or from *E* to *H*. All sections are counterstained with hematoxylin. Cell bodies of Purkinje cells are indicated by asterisks. GL, Granular layer; ML, molecular layer. Scale bar, 20 μm.

GluRζ1 synthesis and turnover

The reduced cerebellar contents suggest lowered synthesis or accelerated degradation of GluRζ1 proteins in the absence of GluRε subunits. To address this, transcription, translation, and turnover of the GluRζ1 subunit were compared between wild-type and mutant cerebella.

Transcription and translation levels

Cultured granule cells were prepared from wild-type and mutant cerebella. In this study, mutant granule cells were obtained from the GluRε1-KO mouse, because the GluRε1 subunit is the major subunit at 7–8 d *in vitro* with the GluRε3 subunit at lower abundance (Huh and Wenthold, 1999). Northern blot analysis showed no significant changes in the transcription levels of GluRζ1 mRNA in the wild-type culture (100.0 ± 16.3%; $n = 3$) and GluRε1-KO culture (117.4 ± 41.6%; $n = 3$; $p > 0.05$) (Fig. 7*A*).

Translation activities were compared by a pulse-labeling experiment with [^{35}S]methionine and [^{35}S]cysteine. First, the total GluRζ1 subunit was compared using GluRζ1-pan antibody, and a significant reduction was observed in GluRε1-KO cultures (Fig. 7*B*), 100.0 ± 8.5% in wild-type cultures ($n = 3$) and 61.2 ± 15.5% in GluRε1-KO cultures ($n = 4$; $p < 0.05$). In the same

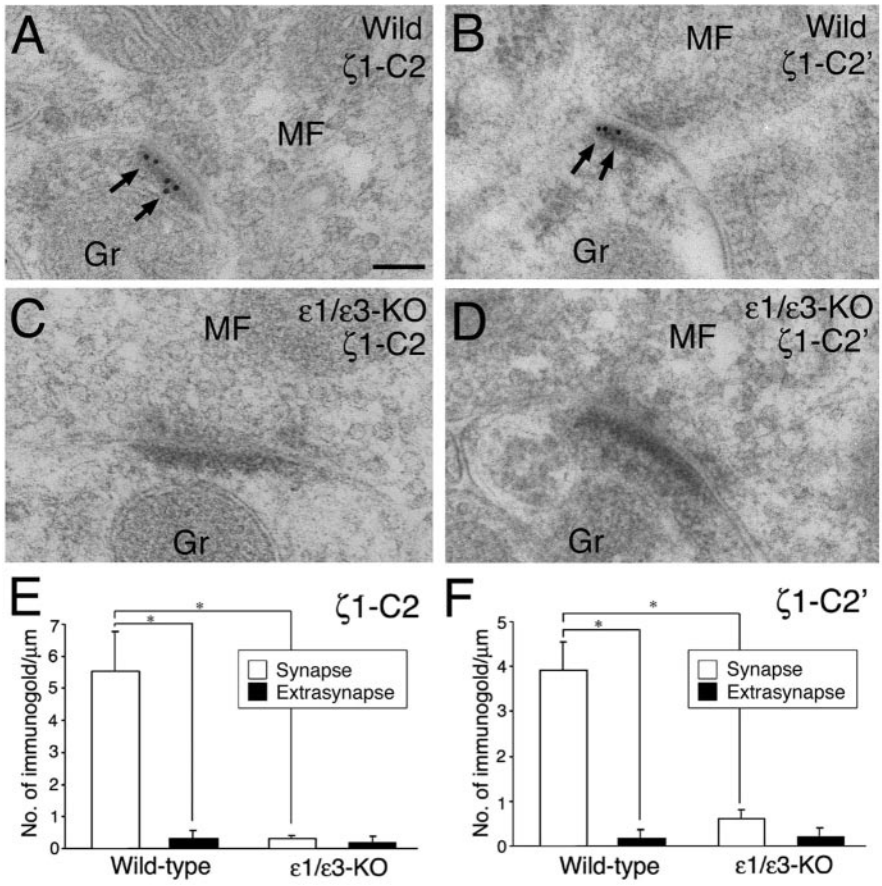

Figure 5. Postembedding immunogold for GluRζ1-C2 (*A*, *C*, *E*) and GluRζ1-C2′ (*B*, *D*, *F*) at mossy fiber–granule cell synapses. Note that postsynaptic labeling for both variants is severely reduced in the GluRε1/ε3-KO mouse (*C*, *D*), in contrast to dense labeling in the wild-type mouse (*A*, *B*, arrows). *E*, *F*, The mean number of immunogold particles per micrometer of synaptic (white columns) and extrasynaptic (black columns) membranes of asymmetrical synapses in the wild-type and GluRε1/ε3-KO mice. Bars on the columns represent the SEM. The asterisks indicate statistically significant differences (Student's *t* test; $p < 0.05$). Gr, Granule cell dendrite; MF, mossy fiber terminal. Scale bar, 100 nm.

cultures, no significant difference was observed for PSD-95 [100.0 ± 3.9% in wild-type cultures and 92.2 ± 4.3% in GluRε1-KO cultures ($p > 0.05$)] (Fig. 7*B*), indicating selective reduction of the GluRζ1 subunit in GluRε1-KO cultures. Then, we immunoprecipitated the GluRζ1 subunit from culture lysates. Immunoblot with the GluRζ1-pan antibody showed that similar amounts of the GluRζ1 subunit were immunoprecipitated from the wild-type (100 ± 18.9%) and GluRε1-KO (102 ± 11.7%) cultures (Fig. 7*C*, top), indicating successful immunoprecipitation by a nonsaturable amount of GluRζ1-pan antibody, as expected. In the immunoprecipitated GluRζ1 subunit, the content of the radioactive (pulse-labeled) GluRζ1 subunit was significantly increased in GluRε1-KO cultures, 100.0 ± 14.9% in wild type and 179.1 ± 73.2% in GluRε1-KO ($p < 0.05$) (Fig. 7*C*, bottom). Because the relative increase of the pulse-labeled GluRζ1 subunit was inversely proportional to the reduction of the total GluRζ1 subunit, the translation of the GluRζ1 subunit in GluRε1-KO cultures was judged to be comparable with that in wild-type cultures. Therefore, the reduced GluRζ1 subunit in the absence of the GluRε subunit is unlikely to result from lowered transcription and translation levels.

Protein turnover analysis

The stability of the GluRζ1 subunit was compared 4 hr after administration of the protein synthesis inhibitor anisomycin (Fig. 7*D*). The reduction in anisomycin-injected mice ($n = 3$) was evaluated as the percentage relative to the levels in vehicle-injected mice ($n = 3$). The total GluRζ1 subunit was reduced mildly to 87.0 ± 17.3% in the wild-type cerebellum but severely to 35.0 ± 0.9% in GluRε1/ε3-KO cerebellum ($p < 0.05$) (Fig. 7*D*,*E*). In contrast, no significant genotypic differences were observed for PSD-95 (109.7 ± 23.9% in the wild type and 88.8 ± 10.9% in the GluRε1/ε3-KO; $p > 0.05$) or synaptophysin (103.3 ± 1.4% in the wild type and 103.8 ± 3.8% in the GluRε1/ε3-KO; $p > 0.05$) (Fig. 7*D*). These results suggest that reduced cerebellar contents of the GluRζ1 subunit thus arise from its accelerated degradation by the ablation of GluRε subunits.

Moreover, different stabilities among GluRζ1 variants were discerned in the GluRε1/ε3-KO mouse. At 4 hr after anisomycin injection, GluRζ1-C2 was reduced severely and significantly to 27.6 ± 8.4% in the mutant mouse compared with 89.8 ± 16.3% in the wild-type mouse ($p < 0.05$) (Fig. 7*D*,*E*). In contrast, the reduction of GluRζ1-C2′ was moderate [66.5 ± 14.7% in the GluRε1/ε3-KO mouse and 82.1 ± 30.0% in the wild-type mouse ($p > 0.05$)] (Fig. 7*D*,*E*). Therefore, GluRζ1-C2 is subjected to more rapid degradation than GluRζ1-C2′, when GluRε subunits are lacking.

Cerebellar anatomy

To finally address whether these alterations arose, at least in part, from abnormal cellular and synaptic differentiation in granule cells, the anatomy of the GluRε1/ε3-KO cerebellum ($n = 3$) was compared with that of the wild-type cerebellum ($n = 3$) (Fig. 8). No histological differences were noted in size, lobule formation, or laminated structure of the cerebellum (Fig. 8*A*,*B*, insets). This was confirmed by measurement of the mean area of the granular layer, using midsagittal cerebellar sections [2.45 ± 0.08 mm^2 in the wild-type mouse and 2.56 ± 0.12 mm^2 in the GluRε1/ε3-KO mouse, showing no significant difference (mean ± SEM; Student's *t* test; $p > 0.05$)]. By morphometric measurement for granule cell nuclei (Fig. 8*A*,*B*), the density of granule cells was estimated to be 3.86 ± 0.56 in the wild-type mouse and 3.77 ± 0.30 ($\times 10^6/mm^3$ of the granular layer) in the GluRε1/ε3-KO mouse, showing no significant difference ($p > 0.05$). Electron microscopy revealed that asymmetrical synapses between huge mossy fiber terminals and digits of granule cell dendrites were normally formed and organized into synaptic glomeruli (Fig. 8*C*,*D*). No significant difference was seen in the length of PSD at mossy fiber–granule cell synapses, being 243 ± 33 nm in the wild-type mouse ($n = 3$; 100 PSDs) and 248 ± 8 nm in the GluRε1/ε3-KO mouse ($n = 3$; 120 PSDs; $p > 0.05$). Double immunofluorescence for vesicular glutamate transporter VGluT1 and vesicular GABA transporter VGAT demonstrated normal organization of excitatory and inhibitory afferents into synaptic glomeruli (Fig. 8*E*,*F*): in both mice, VGluT1-positive

terminals (i.e., mossy fiber terminals, red) were located centrally, whereas VGAT-positive terminals (Golgi cell terminals, green) were located peripherally and surrounded the former.

Therefore, impaired synaptic localization and accelerated turnover of the GluRζ1 subunit is unlikely to result from developmental defects in the cerebellar anatomy and circuitry.

Discussion

In the present study, we produced animal models with cerebellar granule cells lacking major GluRε subunits, GluRε1 and GluRε3, and examined changes in the expression, distribution, and localization of the GluRζ1 subunit. The most notable change emerged in the immunochemical visibility of the GluRζ1 subunit in the cerebellar granular layer. The order of immunohistochemical loss is grossly parallel with that in a previous electrophysiological study in which NMDA receptor-mediated currents are significantly reduced in granule cells lacking the GluRε1 or GluRε3 subunit, and almost absent in those lacking both subunits (Kadotani et al., 1996). The loss of the GluRζ1 subunit is attributable to neither transcriptional and translational downregulations nor to abnormal cellular and synaptic differentiations of granule cells. This results from impaired synaptic localization and protein stability of the GluRζ1 subunit in the absence of GluRε subunits, as follows.

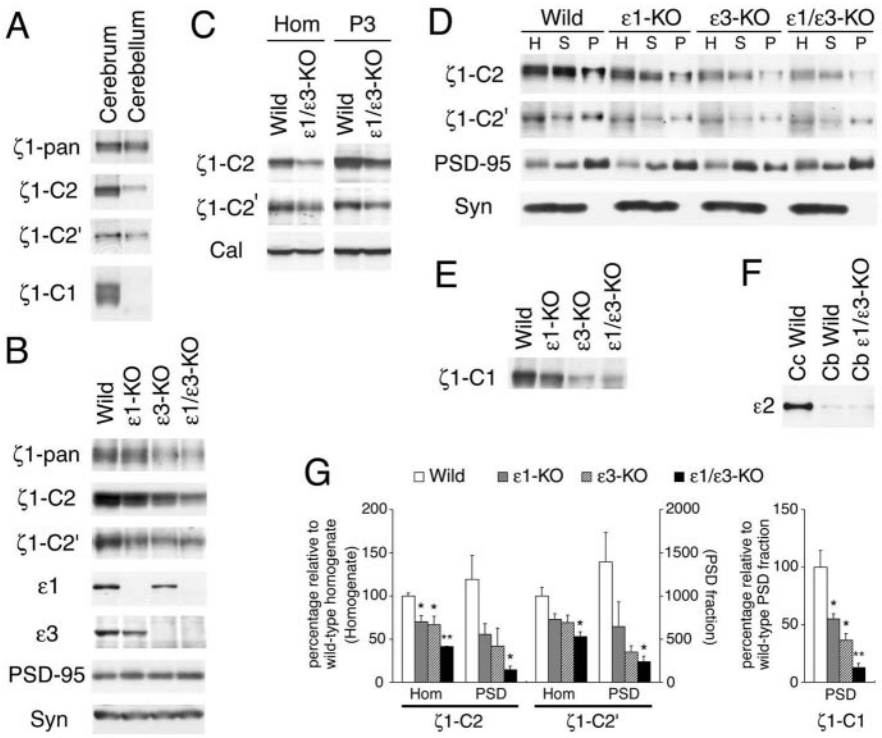

Figure 6. Immunoblot analysis. *A*, GluRζ1 subunit in wild-type cerebral and cerebellar homogenates. The proteins loaded in lanes for total GluRζ1 (ζ1-pan), GluRζ1-C2, and GluRζ1-C2′ are 10 μg for the cerebrum and 30 μg for the cerebellum, and those for GluRζ1-C1 are 30 and 50 μg, respectively. *B*, Cerebellar contents of GluRζ1, GluRε1, GluRε3, PSD-95, and synaptophysin in the wild-type, GluRε1-KO, GluRε3-KO, and GluRε1/ε3-KO mice. Each lane contains 30 μg of proteins. *C*, GluRζ1-C2, GluRζ1-C2′, or calreticulin levels in homogenates (Hom) and P3 fraction (P3) prepared from the wild-type and GluRε1/ε3-KO cerebella. Each lane contains 30 μg of proteins. *D*, GluRζ1-C2, GluRζ1-C2′, PSD-95, or synaptophysin levels in homogenates (H), synaptosomal fraction (S), and PSD fraction (P) in the wild-type, GluRε1-KO, GluRε3-KO, and GluRε1/ε3-KO mice. The proteins loaded in each lane are 30 μg for homogenates, 10 μg for the synaptosomal fraction, and 3 μg for the PSD fraction. *E*, GluRζ1-C1 levels in the PSD fraction. Each lane contains 10 μg of PSD fraction proteins. *F*, GluRε2 levels in homogenates prepared from the wild-type cerebral cortex (Cc, Wild) and from the cerebellum of the wild-type (Cb, Wild) or GluRε1/ε3-KO (Cb, ε1/ε3-KO) mouse. The proteins loaded in each lane are 10 μg for the cerebral cortex and 30 μg for the cerebellum. *G*, Histograms showing progressive loss of GluRζ1 proteins in mutant cerebella. The left histograms show the percentage of GluRζ1-C2 and GluRζ1-C2′ levels in the mutant cerebellar homogenates (see left ordinate) and PSD fraction (see right ordinate) relative to the levels in wild-type cerebellar homogenates (mean ± SEM). The right histograms show the percentage of GluRζ1-C1 levels in the PSD fraction of mutant cerebella relative to the level in wild-type PSD fraction (mean ± SEM). The statistical difference relative to the wild-type levels in each fraction was determined by a Student's unpaired *t* test (*$p < 0.05$; **$p < 0.01$).

GluRε subunits are essential for postsynaptic localization of the GluRζ1 subunit

In light microscopic immunohistochemistry, GluRζ1-C2 and GluRζ1-C2′ were concentrated in synaptic glomeruli in the wild-type cerebellum and were progressively reduced in the GluRε-deficient cerebella. By postembedding immunogold, both variants were localized selectively on the postsynaptic membrane at mossy fiber–granule cell synapses and disappeared almost completely in the GluRε1/ε3-KO mouse. By immunoblot with fractionated protein samples, the most severe deficit of the GluRζ1 subunit was observed in the PSD fraction of the GluRε1/ε3-KO mouse, with the level relative to the wild-type PSD fraction being 12.3% for GluRζ1-C2, 17.0% for GluRζ1-C2′, and 12.7% for GluRζ1-C1. Considering that the cerebellum at 1 month of age contains trace or low levels of the GluRε2 (Fig. 6*C*) and GluRε4 (our unpublished data) subunits as well, the remaining GluRζ1 subunit in the PSD fraction would have reduced more severely, if all four GluRε subunits are thoroughly ablated. Based on these findings, the first conclusion of the present study is that GluRε subunits are the major molecular determinant for postsynaptic localization of the GluRζ1 subunit regardless of its C-terminal forms, at least, in cerebellar granule cells. This notion is compatible with our previous observation on immunohistochemical invisibility of the GluRζ1 subunit in adult wild-type Purkinje cells (Yamada et al., 2001), in which GluRζ1 mRNA is highly expressed but none of the GluRε subunits are transcribed (Watanabe et al., 1994). Thus, GluRε-dependent synaptic localization of the GluRζ1 subunit seems general to various neurons.

The C terminus of GluRε subunits interacts strongly and specifically with PDZ domain proteins in the PSD, such as PSD-95, SAP-102, and Chapsyn-110 (Kornau et al., 1995; Niethammer et al., 1996; Wyszynski et al., 1997; Ehlers et al., 1998). C-terminal truncation of the GluRε1 or GluRε2 subunit has reduced the amount of synaptic NMDA receptors in hippocampal pyramidal cells (Mori et al., 1998; Steigerwald et al., 2000). Although synaptic localization of NMDA receptors is not impaired in mutant mice lacking PSD-95 (Migaud et al., 1998), the interaction of C termini of GluRε subunits with multiple members of the PSD protein family is a likely mechanism for the GluRε-dependent postsynaptic localization of the GluRζ1 subunit.

GluRε subunits increase protein stability of the GluRζ1 subunit

There is a large cytoplasmic pool for the GluRζ1 subunit (Hall and Soderling, 1997). This pool, being obtained as Triton X-100-

Table 1. Relative concentrations of GluRζ1 proteins in subcellular fractions of the wild-type and mutant cerebella

Protein	Genotype	Homogenate	Synaptosome	PSD fraction
GluRζ1-pan	Wild type	100.0 ± 8.4	—	—
	ε1-KO	74.0 ± 15.8	—	—
	ε3-KO	69.6 ± 13.2	—	—
	ε1/ε3-KO	60.3 ± 10.2*	—	—
GluRζ1-C2	Wild type	100.0 ± 3.2	100 ± 23.0	100 ± 23.3
	ε1-KO	70.2 ± 7.1*	62.4 ± 7.6	46.6 ± 10.5
	ε3-KO	66.5 ± 10.1*	71.5 ± 12.6	35.0 ± 17.7
	ε1/ε3-KO	41.4 ± 0.4**	34.2 ± 5.6*	12.3 ± 3.3*
GluRζ1-C2′	Wild type	100.0 ± 9.6	100 ± 10.5	100 ± 24.4
	ε1-KO	73.1 ± 6.4	47.9 ± 12.8*	46.2 ± 20.6
	ε3-KO	69.1 ± 8.6	60.5 ± 17.2	25.1 ± 5.3
	ε1/ε3-KO	53.0 ± 5.6*	26.3 ± 4.3**	17.0 ± 4.6*
GluRζ1-C1	Wild type	ND	—	100 ± 14.5
	ε1-KO	ND	—	55.2 ± 4.3*
	ε3-KO	ND	—	36.6 ± 5.7*
	ε1/ε3-KO	ND	—	12.7 ± 3.5**

Each value was calculated from the signals of immunoblot bands and is relative to the value of wild-type cerebellum in each fraction. All data are given as the mean ± SEM for three experiments, except for GluRζ1-C2′ proteins of the wild-type mouse ($n = 5$) and the GluRζ1-C1 protein of the wild-type PSD fraction ($n = 4$). Genotypic differences relative to wild-type scores within respective sample fractions were statistically determined by Student's t test. *$p < 0.05$; **$p < 0.01$. —, Not tested; ND, not detectable.

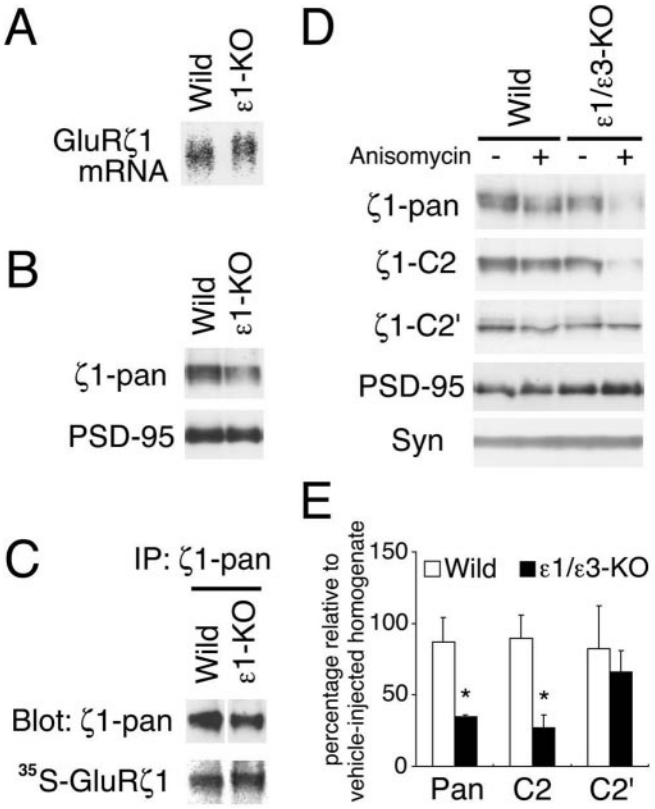

Figure 7. Transcription, translation, and protein turnover analyses for the GluRζ1 subunit. *A*, Northern blot analysis for GluRζ1 mRNA in the wild-type and GluRε1-KO cerebellar cultures. The total RNA loaded in each lane is 5 μg. *B*, Immunoblot with GluRζ1-pan and PSD-95 antibodies for cell lysates from wild-type and GluRε1-KO cerebellar cultures. Each lane contains 30 μg of proteins. *C*, Pulse-labeling experiment. After pulse-labeling with [^{35}S]Met/Cys for 30 min, cell lysates were immunoprecipitated with GluRζ1-pan antibody. Immunoprecipitates were then analyzed to compare the amount of precipitated GluRζ1 subunit by immunoblot (Blot: ζ1-pan) and to compare the radioactivity of pulse-labeled GluRζ1 subunit (^{35}S-GluRζ1). *D*, Protein stability experiment at 4 hr after anisomysin injection to the wild-type and GluRε1/ε3-KO mice. Cerebellar homogenates from vehicle-injected (−) and anisomycin-injected (+) mice were immunoreacted with GluRζ1-pan, GluRζ1-C2, GluRζ1-C2′, PSD-95, or synaptophysin antibody. *E*, Histograms showing different stabilities among total GluRζ1 subunit (pan), GluRζ1-C2, and GluRζ1-C2′ in anysomicin-injected cerebellar homogenates. Values are expressed as the percentage of the protein levels relative to those from vehicle-injected homogenates in each mouse type (mean ± SEM). The statistical difference in the reduction between the wild-type and GluRε1/ε3-KO mice was determined by a Student's unpaired t test (*$p < 0.05$).

solubilized P3 fraction, represents an unassembled, monomeric GluRζ1 subunit (Chazot and Stephenson, 1997). Turnover analysis has further demonstrated biphasic decay of the [^{35}S]methionine-labeled GluRζ1 subunit with half-lives of 2 and 34 hr (Huh and Wenthold, 1999). Of the two, the slowly degraded (or stable) pool represents the GluRζ1 subunit on the cell surface, whereas the rapidly degraded pool represents an unassembled GluRζ1 subunit in the cytoplasm. From this *in vitro* evidence, we had supposed that the cytoplasmic pool would increase with reciprocal decrease of the surface/synaptic pool in the GluRε-deficient cerebella.

Contrary to our presumption, GluRζ1-C2 and GluRζ1-C2′ in the GluRε1/ε3-KO cerebellum were reduced not only in the synaptosomal and PSD fractions but also in the P3 fraction to 60–64%. This result led us to assume that before becoming the cytoplasmic and surface/synaptic pools, a fraction of the GluRζ1 subunit undergoes more rapid, premature degradation and that this might have increased in the GluRε-deficient cerebella. To test this, we used protein turnover analysis. At 4 hr after anisomycin injection, the total GluRζ1 subunit relative to the level after vehicle injection was severely reduced in the GluRε1/ε3-KO cerebellum (35.0%), whereas it decreased mildly in the wild-type cerebellum (87.9%). Therefore, the second conclusion of the present study is that accompanying GluRε subunits enhance protein stability of the GluRζ1 subunit, leading to increases of both the cytoplasmic and synaptic pools. The enhanced protein stability appears to be linked, at least in part, with the formation of heteromeric NMDA receptors in the ER because coexpression of GluRζ1 and GluRε subunits greatly promotes the export of the GluRζ1 subunit from the ER to the cell surface (McIlhinney et al., 1996, 1998) and to the postsynaptic site (the present study). The premature degradation of the GluRζ1 subunit is probably conducted as either ER-associated degradation in the ER or ubiquitin–proteasomal degradation in the cytoplasm (Johnston et al., 1998; Fukaya et al., 2003).

C terminus-dependent self-ER export mechanisms in neurons *in vivo*

Relatively higher uses of the C2′ cassette in the cerebellum and of the C1 and C2 cassettes in the cerebral cortex are generally consistent with previous studies by *in situ* hybridization and immunoblot analyses (Laurie and Seeburg, 1994; Al-Hallaq et al., 2001). In the present study, C-terminal cassette-dependent differences of the GluRζ1 subunit were also appreciated in the brain *in vivo*. A notable difference was seen in protein stability between GluRζ1-C2 and GluRζ1-C2′ when GluRε subunits were lacking. Four hours after anisomycin injection, GluRζ1-C2 was reduced severely to 27.6%, whereas GluRζ1-C2′ was mildly reduced to 66.5% in the GluRε1/ε3-KO mouse, suggesting a different turnover rate depending on the C2/C2′ form. Unfortunately, how GluRζ1-C1 is stable in the absence of GluRε subunits was not addressed in the present study because of its particularly low contents in the cerebellum.

The C-terminal cassette-related difference in the protein stability appears to be concerned with C terminus-dependent self-ER export mechanisms. When transfected to heterologous cells *in vitro*, the GluRζ1 subunit ended with a C1–C2 tail (i.e.,

NR1–1 or $NR1_{X11}$) is lowest in the cell surface expression and extensively accumulates intracellularly, whereas the splice variant lacking the C1 cassette and ended with a C2′ tail (NR1–4 or $NR1_{X00}$) displays the highest surface expression (McIlhinney et al., 1996; Okabe et al., 1999). As the underlying mechanisms, particular domains in the C2′ tail have been shown to facilitate forward ER trafficking to the cell surface. One is by the PDZ-interacting domain in the C2′ tail, which mediates self-suppression of the ER retention motif RXR residing in the C1 cassette (Standley et al., 2000; Scott et al., 2001), and the other is by the TVV export motif in the C2′ tail, which recruits NMDA receptors to ER exit sites (Mu et al., 2003). Taking this evidence from *in vitro* studies into our observations, the higher protein stability of GluRζ1-C2′ than GluRζ1-C2 can be interpreted that more efficient ER export for the former might have prolonged its turnover rate. Therefore, the C terminus-dependent self-ER export system seems functional in neurons *in vivo*, when accompanying GluRε subunits are lacking. Considering the fact that most central neurons coexpress GluRζ1 and one or more GluRε subunits (Watanabe et al., 1993, 1994), the C terminus-dependent self-ER export mechanisms for GluRζ1 subunit would be suppressed or masked by the strong action of GluRε-dependent cell surface delivery and synaptic localization for the GluRζ1 subunit.

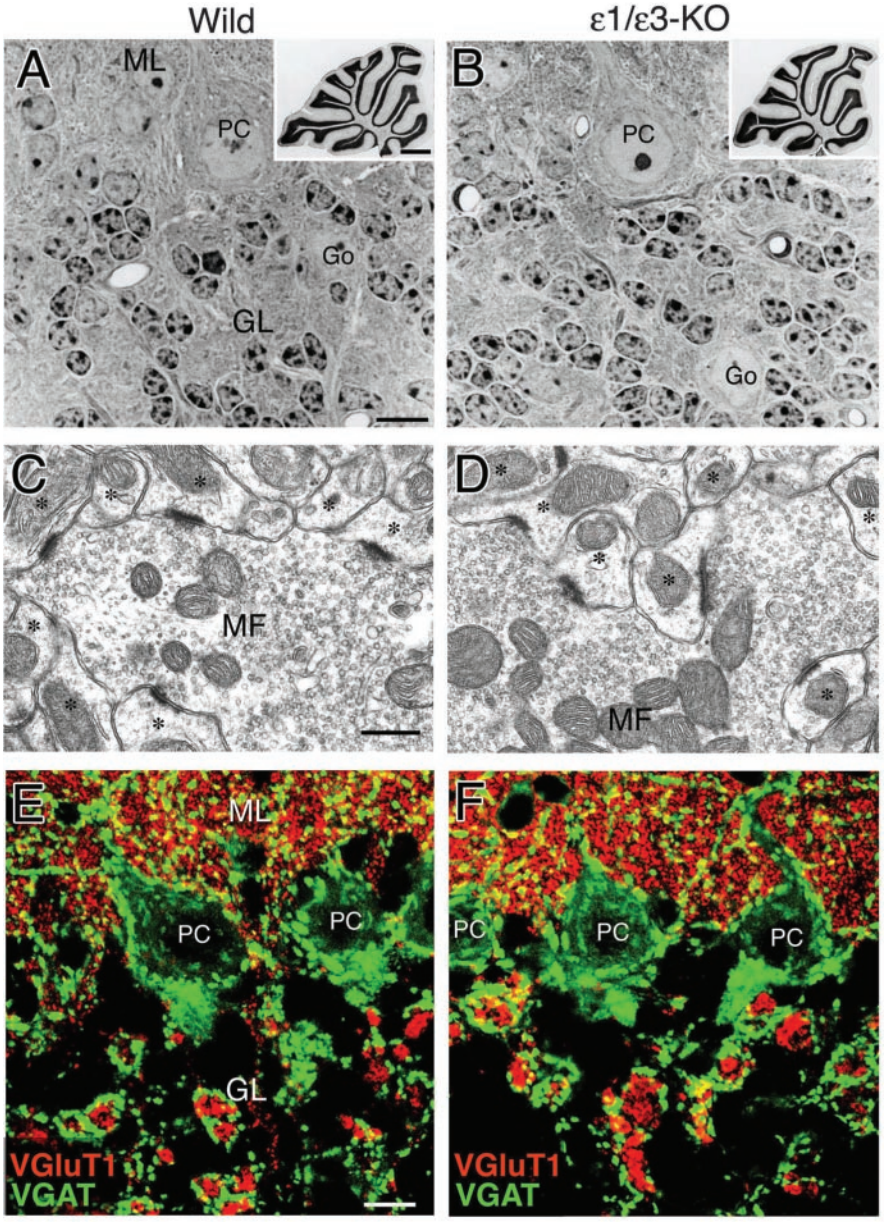

Figure 8. Anatomical and synaptic organization of the wild-type (*A*, *C*, *E*) and GluRε1/ε3-KO (*B*, *D*, *F*) cerebella. *A*, *B*, Normal cytoarchitecture of the cerebellar cortex is shown by hematoxylin-stained Epon semithin sections. Normal cerebellar histoarchitecture is also shown by hematoxylin-stained microslicer sections (insets). *C*, *D*, Electron micrographs showing huge mossy fiber terminals (MF) forming asymmetrical synapses with granule cell dendrites (asterisk). *E*, *F*, Double immunofluorescence for vesicular glutamate transporter VGluT1 (red) and vesicular GABA transporter VGAT (green) in the cerebellar cortex. GL, Granular layer; Go, Golgi cell; ML, molecular layer; PC, Purkinje cell. Scale bars: *A*, 10 μm (inset, 1 mm); *C*, 0.2 μm; *E*, 10 μm.

Facilitative interaction between GluRε subunits

We noticed reduced immunohistochemical and immunblot levels for the GluRε1 or GluRε3 subunit in the absence of the other. This suggests that facilitative interaction also works among GluRε subunits, which would lead to the increase of receptor complex formation or protein stability. This notion is in line with a finding that the availability of GluRε subunits, but not the GluRζ1 subunit, determines the total number of functional NMDA receptors in cultured cerebellar granule cells (Prybylowski et al., 2002).

Through our present and previous analyses using the *in vivo* system, it is evident that synaptic expression of NMDA receptors is regulated by GluRζ1 and GluRε subunits in a different but cooperative manner. In the absence of GluRε subunits, the GluRζ1 subunit is unable to be localized on the postsynapse, regardless of its C-terminal forms. Without the GluRζ1 subunit, GluRε subunits are obliged to undergo ER retention (Fukaya et al., 2003). These dual mechanisms will constitute strict quality control mechanisms by which heteromeric NMDA receptors constructed properly are only permitted to be expressed on the postsynapse.

References

Al-Hallaq RA, Yasuda RP, Wolfe BB (2001) Enrichment of *N*-methyl-D-aspartate NR1 splice variants and synaptic proteins in rat postsynaptic densities. J Neurochem 77:110–119.

Bliss TV, Collingridge GL (1993) A synaptic model of memory: long-term potentiation in the hippocampus. Nature 361:31–39.

Carlin RK, Grab DJ, Cohen RS, Siekevitz P (1980) Isolation and characterization of postsynaptic densities from various brain regions: enrichment of different types of postsynaptic densities. J Cell Biol 86:831–845.

Chazot PL, Stephenson FA (1997) Biochemical evidence for the existence of a pool of unassembled C2 exon-containing NR1 subunits of the mammalian forebrain NMDA receptor. J Neurochem 68:507–516.

Ebralidze AK, Rossi DJ, Tonegawa S, Slater NT (1996) Modification of

NMDA receptor channels and synaptic transmission by targeted disruption of the NR2C gene. J Neurosci 16:5014–5025.
Ehlers MD, Tingley WG, Huganir RL (1995) Regulated subcellular distribution of the NR1 subunit of the NMDA receptor. Science 269:1734–1737.
Ehlers MD, Fung ET, O'Brien RJ, Huganir RL (1998) Splice variant-specific interaction of the NMDA receptor subunit NR1 with neuronal intermediate filaments. J Neurosci 18:720–730.
Fujikawa N, Tominaga-Yoshino K, Okabe M, Ogura A (2000) Depolarization-dependent survival of cultured mouse cerebellar granule neurons is strain-restrained. Eur J Neurosci 12:1838–1842.
Fukaya M, Watanabe M (2000) Improved immunohistochemical detection of postsynaptically located PSD-95/SAP90 protein family by protease section pretreatment: a study in the adult mouse brain. J Comp Neurol 426:572–586.
Fukaya M, Kato A, Lovett C, Tonegawa S, Watanabe M (2003) Retention of NMDA receptor NR2 subunits in the lumen of endoplasmic reticulum in targeted NR1 knockout mice. Proc Natl Acad Sci USA 100:4855–4860.
Hall RA, Soderling TR (1997) Differential surface expression and phosphorylation of the *N*-methyl-D-aspartate receptor subunits NR1 and NR2 in cultured hippocampal neurons. J Biol Chem 272:4135–4140.
Hirai H, Kirsch J, Laube B, Betz H, Kuhse J (1996) The glycine binding site of the *N*-methyl- D-aspartate receptor subunit NR1: identification of novel determinants of co-agonist potentiation in the extracellular M3–M4 loop region. Proc Natl Acad Sci USA 93:6031–6036.
Hollmann M, Boulter J, Maron C, Beasley L, Sullivan J, Pecht G, Heinemann S (1993) Zinc potentiates agonist-induced currents at certain splice variants of the NMDA receptor. Neuron 10:943–954.
Huh K-H, Wenthold RJ (1999) Turnover analysis of glutamate receptors identifies a rapidly degraded pool of the *N*-methyl- D-aspartate receptor subunit, NR1, in cultured cerebellar granule cells. J Biol Chem 274:151–157.
Johnston JA, Ward CL, Kopito RR (1998) Aggresomes: a cellular response to misfolded proteins. J Cell Biol 143:1883–1898.
Kadotani H, Hirano T, Masugi M, Nakamura K, Nakao K, Katsuki M, Nakanishi S (1996) Motor discoordination results from combined gene disruption of the NMDA receptor NR2A and NR2C subunits, but not from single disruption of the NR2A or NR2C subunit. J Neurosci 16:7859–7867.
Kakizawa S, Yamasaki M, Watanabe M, Kano M (2000) Critical period for activity-dependent synapse elimination in developing cerebellum. J Neurosci 20:4954–4961.
Kornau H-C, Schenker LT, Kennedy MB, Seeburg PH (1995) Domain interaction between NMDA receptor subunits and the postsynaptic density protein PSD-95. Science 269:1737–1740.
Kutsuwada T, Kashiwabuchi N, Mori H, Sakimura K, Kushiya E, Araki K, Meguro H, Masaki H, Kumanishi T, Arakawa M, Mishina M (1992) Molecular diversity of the NMDA receptor channel. Nature 358:36–41.
Lattal KM, Abel T (2001) Different requirements for protein synthesis in acquisition and extinction of spatial preferences and context-evoked fear. J Neurosci 21:5773–5780.
Laube B, Hirai H, Sturgess M, Betz H, Kuhse J (1997) Molecular determinants of agonist discrimination by NMDA receptor subunits: analysis of the glutamate binding site on the NR2B subunit. Neuron 18:493–503.
Laurie DJ, Seeburg PH (1994) Regional and developmental heterogeneity in splicing of the rat brain NMDAR1 mRNA. J Neurosci 14:3180–3194.
Laurie DJ, Putzke J, Zieglgänsberger W, Seeburg PH, Tölle TR (1995) The distribution of splice variants of the NMDAR1 subunit mRNA in adult rat brain. Brain Res Mol Brain Res 32:94–108.
Lin JW, Wyszynski M, Madhavan R, Sealock R, Kim JU, Sheng M (1998) Yotiao, a novel protein of neuromuscular junction and brain that interacts with specific splice variants of NMDA receptor subunit NR1. J Neurosci 18:2017–2027.
Lowry OH, Rosebrough NJ, Farr AL, Randall RJ (1951) Protein measurement with the folin phenol reagent. J Biol Chem 193:265–275.
Matsuda S, Hirai H (1999) The clustering of NMDA receptor NR1 subunit is regulated by the interaction between the C-terminal exon cassettes and the cytoskeleton. Neurosci Res 34:157–163.
Mayer ML, Westbrook GL (1987) The physiology of excitatory amino acids in the vertebrate central nervous system. Prog Neurobiol 28:197–276.
McIlhinney RAJ, Molnár E, Atack JR, Whiting PJ (1996) Cell surface expression of the human *N*-methyl- D-aspartate receptor subunit 1a requires the co-expression of the NR2A subunit in transfected cells. Neuroscience 70:989–997.
McIlhinney RAJ, Le Bourdellés B, Molnár E, Tricaud N, Streit P, Whiting PJ (1998) Assembly intracellular targeting and cell surface expression of the human *N*-methyl-D-aspartate receptor subunits NR1a and NR2A in transfected cells. Neuropharmacology 37:1355–1367.
Meguro H, Mori H, Araki K, Kushiya E, Kutsuwada T, Yamazaki M, Kumanishi T, Arakawa M, Sakimura K, Mishina M (1992) Functional characterization of a heteromeric NMDA receptor channel expressed from cloned cDNAs. Nature 357:70–74.
Migaud M, Charlesworth P, Dempster M, Webster LC, Watabe AM, Makhinson M, He Y, Ramsay MF, Morris RG, Morrison JH, O'Dell TJ, Grant SG (1998) Enhanced long-term potentiation and impaired learning in mice with mutant postsynaptic density-95 protein. Nature 396:433–439.
Miyazaki T, Fukaya M, Shimizu H, Watanabe M (2003) Subtype switching of vesicular glutamate transporters at parallel fiber-Purkinje cell synapses in developing mouse cerebellum. Eur J Neurosci 17:2563–2572.
Monyer H, Sprengel R, Schoepfer R, Herb A, Higuchi M, Lomeli H, Burnashev N, Sakmann B, Seeburg PH (1992) Heteromeric NMDA receptors: molecular and functional distinction of subtypes. Science 256:1217–1221.
Mori H, Mishina M (1995) Structure and function of the NMDA receptor channel. Neuropharmacology 34:1219–1237.
Mori H, Manabe T, Watanabe M, Satoh Y, Suzuki N, Toki S, Nakamura K, Yagi T, Kushiya E, Takahashi T, Inoue Y, Sakimura K, Mishina M (1998) Role of the carboxy-terminal region of the GluRε2 subunit in synaptic localization of the NMDA receptor channel. Neuron 21:571–580.
Mu Y, Otsuka T, Horton AC, Scott DB, Ehlers MD (2003) Activity-dependent mRNA splicing controls ER export and synaptic delivery of NMDA receptors. Neuron 40:581–594.
Nagasawa M, Sakimura K, Mori KJ, Bedell MA, Copeland NG, Jenkins NA, Mishina M (1996) Gene structure and chromosomal localization of the mouse NMDA receptor channel subunits. Brain Res Mol Brain Res 36:1–11.
Nakanishi S, Masu M (1994) Molecular diversity and functions of glutamate receptors. Annu Rev Biophys Biomol Struct 23:319–348.
Niethammer M, Kim E, Sheng M (1996) Interaction between the C terminus of NMDA receptor subunits and multiple members of the PSD-95 family of membrane-associated guanylate kinases. J Neurosci 16:2157–2163.
Okabe S, Miwa A, Okado H (1999) Alternative splicing of the C-terminal domain regulates cell surface expression of the NMDA receptor NR1 subunit. J Neurosci 19:7781–7792.
Oshima S, Fukaya M, Masabumi N, Shirakawa T, Oguchi H, Watanabe M (2002) Early onset of NMDA receptor GluRε1 (NR2A) expression and its abundant postsynaptic localization in developing motoneurons of the mouse hypoglossal nucleus. Neurosci Res 43:239–250.
Prybylowski K, Fu Z, Losi G, Hawkins LM, Luo J, Chang K, Wenthold RJ, Vicini S (2002) Relationship between availability of NMDA receptor subunits and their expression at the synapse. J Neurosci 22:8902–8910.
Sakimura K, Kutsuwada T, Ito I, Manabe T, Takayama C, Kushiya E, Yagi T, Aizawa S, Inoue Y, Sugiyama H, Mishina M (1995) Reduced hippocampal LTP and spatial learning in mice lacking NMDA receptor ε1 subunit. Nature 373:151–155.
Scott DB, Blanpied TA, Swanson GT, Zhang C, Ehlers MD (2001) An NMDA receptor ER retention signal regulated by phosphorylation and alternative splicing. J Neurosci 21:3063–3072.
Seeburg PH (1993) The molecular biology of mammalian glutamate receptor channels. Trends Neurosci 16:359–365.
Setou M, Nakagawa T, Seog D-H, Hirokawa N (2000) Kinesin superfamily motor protein KIF17 and mLin-10 in NMDA receptor-containing vesicle transport. Science 288:1796–1802.
Standley S, Roche KW, McCallum J, Sans N, Wenthold RJ (2000) PDZ domain suppression of an ER retention signal in NMDA receptor NR1 splice variants. Neuron 28:887–898.
Steigerwald F, Schulz TW, Schenker LT, Kennedy MB, Seeburg PH, Köhr G (2000) C-Terminal truncation of NR2A subunits impairs synaptic but not extrasynaptic localization of NMDA receptors. J Neurosci 20:4573–4581.
Sugihara H, Moriyoshi K, Ishii T, Masu M, Nakanishi S (1992) Structures and properties of seven isoforms of the NMDA receptor generated by alternative splicing. Biochem Biophys Res Commun 185:826–832.
Takahashi T, Feldmeyer D, Suzuki N, Onodera K, Cull-Candy SG, Sakimura K, Mishina M (1996) Functional correlation of NMDA receptor ε subunits expression with the properties of single-channel and synaptic currents in the developing cerebellum. J Neurosci 16:4376–4382.

Tingley WG, Roche KW, Thompson AK, Huganir RL (1993) Regulation of NMDA receptor phosphorylation by alternative splicing of the C-terminal domain. Nature 364:70–73.

Watanabe M, Inoue Y, Sakimura K, Mishina M (1992) Developmental changes in distribution of NMDA receptor channel subunit mRNAs. NeuroReport 3:1138–1140.

Watanabe M, Inoue Y, Sakimura K, Mishina M (1993) Distinct distributions of five *N*-methyl-D-aspartate receptor channel subunit mRNAs in the forebrain. J Comp Neurol 338:377–390.

Watanabe M, Mishina M, Inoue Y (1994) Distinct spatiotemporal expressions of five NMDA receptor channel subunit mRNAs in the cerebellum. J Comp Neurol 343:513–519.

Watanabe M, Fukaya M, Sakimura K, Manabe T, Mishina M, Inoue Y (1998) Selective scarcity of NMDA receptor channel subunits in the stratum lucidum (mossy fibre-recipient layer) of the mouse hippocampal CA3 subfield. Eur J Neurosci 10:478–487.

Weibel ER (1979) Practical methods for biological morphometry. In: Stereological methods I (Weibel ER, ed), pp 101–161. New York: Academic.

Wyszynski M, Lin J, Rao A, Nigh E, Beggs AH, Craig AM, Sheng M (1997) Competitive binding of α-actinin and calmodulin to the NMDA receptor. Nature 385:439–442.

Yagi T, Nada S, Watanabe N, Tamemoto H, Kohmura N, Ikawa Y, Aizawa S (1993) A novel negative selection for homologous recombinants using diphtheria toxin A fragment gene. Anal Biochem 214:77–86.

Yamada K, Fukaya M, Shimizu H, Sakimura K, Watanabe M (2001) NMDA receptor subunits GluRε1, GluRε3 and GluRζ1 are enriched at the mossy fibre-granule cell synapse in the adult mouse cerebellum. Eur J Neurosci 13:2025–2036.

Yamazaki M, Mori H, Araki K, Mori KJ, Mishina M (1992) Cloning, expression and modulation of a mouse NMDA receptor subunit. FEBS Lett 300:39–45.

Yanagawa Y, Kobayashi T, Ohnishi M, Kobayashi T, Tamura S, Tsuzuki T, Sanbo M, Yagi T, Tashiro F, Miyazaki J (1999) Enrichment and efficient screening of ES cells containing a targeted mutation: the use of DT-A gene with the polyadenylation signal as a negative selection maker. Transgenic Res 8:215–221.